BIOCHEMISTRY
including biophysical chemistry & molecular biology
Accelerated Publication

Biochemistry **2009,** *48,* 6705–6711 6705
DOI: 10.1021/bi900850y

Identification of *Escherichia coli* HemG as a Novel, Menadione-Dependent Flavodoxin with Protoporphyrinogen Oxidase Activity†

Tye O. Boynton, Lauren E. Daugherty, Tamara A. Dailey, and Harry A. Dailey*

Biomedical and Health Sciences Institute and Department of Microbiology, University of Georgia, Athens, Georgia 30602

Received May 19, 2009; Revised Manuscript Received June 26, 2009

ABSTRACT: Protoporphyrinogen oxidase (PPO, EC 1.3.3.4) catalyzes the six-electron oxidation of protoporphyrinogen IX to the fully conjugated protoporphyrin IX. Eukaryotes and Gram-positive bacteria possess an oxygen-dependent, FAD-containing enzyme for this step, while the majority of Gram-negative bacteria lack this oxygen-dependent PPO. In *Escherichia coli*, PPO activity is known to be linked to respiration and the quinone pool. In *E. coli* SASX38, the knockout of *hemG* causes a loss of measurable PPO activity. HemG is a small soluble protein typical of long chain flavodoxins. Herein, purified recombinant HemG was shown to be capable of a menadione-dependent conversion of protoporphyrinogen IX to protoporphyrin IX. Electrochemical analysis of HemG revealed similarities to other flavodoxins. Interestingly, HemG, a member of a class of the long chain flavodoxin family that is unique to the γ-proteobacteria, possesses a 22-residue sequence that, when transferred into *E. coli* flavodoxin A, produces a chimera that will complement an *E. coli* hemG mutant, indicating that this region confers PPO activity to the flavodoxin. These findings reveal a previously unidentified class of PPO enzymes that do not utilize oxygen as an electron acceptor, thereby allowing γ-proteobacteria to synthesize heme in both aerobic and anaerobic environments.

Heme is a highly versatile small organic compound that is a key component of most living organisms. As a cofactor, it functions in diverse reactions ranging from a gas sensor and transporter of diatomic gases to an electron carrier in redox-linked reactions such as those found in mixed-function oxidases, catalases, or electron transport chains (*1*−*3*). In addition, it is now recognized that it is also a regulatory molecule. It has been shown to manage protein expression at the transcriptional (*4*, *5*) and translational levels (*6*) as well as through protein targeting and degradation (*7*); it participates in regulating circadian rhythm, lipid metabolism, and gluconeogenesis (*8*−*10*), and in prokaryotic organisms, heme may even serve to alter pathogenesis by triggering decreased virulence levels and evasion of the host immune response (*11*, *12*).

The biosynthesis of heme has been studied in both eukaryotes and prokaryotes. It is a tightly regulated metabolic pathway consisting of seven enzymatic steps from a precursor compound 5-aminolevulinic acid to the end product, protoheme (*13*). In humans and animals, defects in any of these seven enzymes result in clinically distinct diseases, porphyrias, due to an accumulation of pathway intermediates (*14*). While the system has been extensively studied and is relatively well understood in eukaryotes (*15*), the pathway is less well-defined in bacteria and archaea (*16*). Two steps in particular, the penultimate and antepenultimate, have characterized enzymes that require molecular oxygen as an electron acceptor in eukaryotes. In higher organisms and a handful of Gram-negative organisms such as *Myxococcus xanthus*, the penultimate enzyme, protoporphyrinogen oxidase (PPO), exists as a membrane-associated enzyme that utilizes an FAD cofactor (*17*, *18*) and converts oxygen to hydrogen peroxide during the reaction (Scheme 1). This enzyme belongs to an FAD superfamily of proteins that also contains monoamine oxidases and phytoene desaturases (*19*). A soluble form of the enzyme named HemY is found in Gram-positive bacteria that produce heme, and apart from its solubility, it is virtually the same as the eukaryotic enzyme (*20*). Not surprisingly, these oxygen-dependent enzymes have not been found in facultative or anaerobic bacteria, although it is clear that some mechanism for catalyzing this reaction must exist.

Investigations by the Jacobs group in the 1970s found that PPO enzymatic activity was found in crude cellular extracts of *Escherichia coli* and was reported to be membrane-associated (*21*). The activity was intimately linked to cellular respiration and increased in the presence of a terminal electron acceptor such as fumarate or nitrate (*22*−*24*). Respiratory enzymes using these substrates all share one thing in common: the usage of quinones, specifically menaquinone-8, as electron donors (*25*, *26*). These same studies also showed that menaquinone-deficient *E. coli* were deficient in PPO activity (*21*). Mutagenesis of *E. coli* by the Sasarman group resulted in the production of one mutant, SASX38, that was deficient in PPO activity (*27*). The gene, named *hemG*, was mapped and later annotated as being responsible for the penultimate step in heme biosynthesis (*28*). Sequence analysis of the encoded protein reveals it to be a member of the protein family known as long chain flavodoxins. These are small electron transfer proteins containing an FMN cofactor. They are distinct from the small chain flavodoxins in that they possess an additional loop inserted in the fifth β-strand. This insert has previously been implicated in specificity and function between redox partners (*29*, *30*). To date, however, there are no published data for the expression, purification, and characterization of HemG. Of particular note, because of HemG's resemblance to flavodoxins, it has been generally assumed that it may simply function as

†This work was supported by National Institutes of Health Grant DK32303 to H.A.D.

*To whom correspondence should be addressed: 500 D. W. Brooks Dr., Athens, GA 30605. Telephone: (706) 542-2690. Fax: (706) 542-5285. E-mail: hdailey@uga.edu.

Published on Web 06/29/2009

Scheme 1: Reaction Catalyzed by Oxygen-Dependent Protoporphyrinogen Oxidase

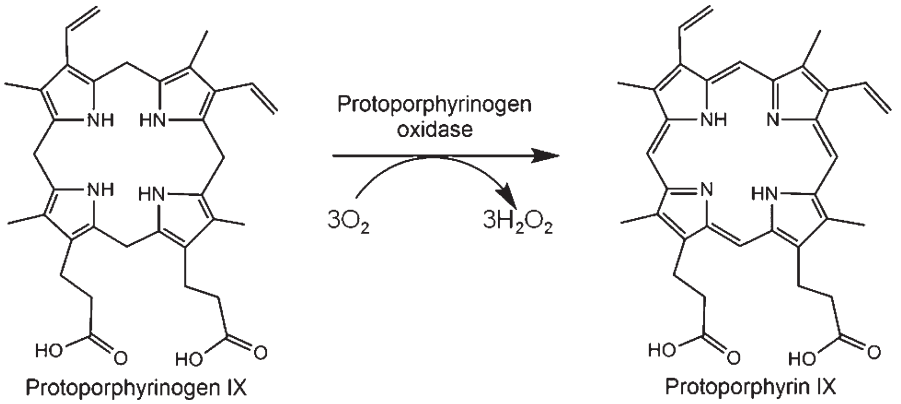

an electron carrier for a bona fide PPO enzyme, and PPO enzymatic activity has never been reported for HemG (*31*).

In this study, the HemG protein was expressed, purified, and characterized. In addition, the nature of the *hemG* mutation in *E. coli* SASX38 was identified. EPR-monitored redox titrations of HemG were performed in examining the FMN cofactor's role in electron transfer, and a menadione-dependent PPO activity was identified and characterized. The possible function for the long chain insert loop, which is unique to HemG of the γ-proteobacteria, was also examined. The data presented unequivocally demonstrate that HemG functions as a protoporphyrinogen oxidase and that the PPO activity is conveyed by the long chain insert loop.

MATERIALS AND METHODS

Bacterial Strains and Constructed Plasmids. The *hemG* gene was amplified from *E. coli* genomic DNA and cloned into the *NheI* and *Hin*dIII sites of the six-His tag vector pTrchisA (Invitrogen, Carlsbad, CA). The resulting plasmid, pTHHemG, was then tested for functionality via transformation into the SASX38 cell line that contains a knockout of *hemG*. Overexpression of the recombinant protein was conducted in JM109 cells. *Bdellovibrio bacteriovorus Bd2899* was cloned in a manner identical to that of *E. coli hemG*. The chimeric FldG plasmid was constructed by first cloning the *fldA* gene of *E. coli* into pTrchisA, and then Quickchange (Stratagene, Jolla, CA) mutagenesis was used to swap the 66-nucleotide insert region with that of *hemG*.

Protein Expression, Purification, and Characterization. Cells containing pTHHemG were grown for 7 h at 30 °C in 100 mL of Circlegrow (MP Biomedicals, Solon, OH) containing 50 μg/mL ampicillin, transferred to 1 L of the same medium, and grown for 22 h at 30 °C. Six hours prior to being harvested, the cells were supplemented with riboflavin at a final concentration of 0.75 mg/mL. Cells were then collected by centrifugation and resuspended in a solubilization buffer containing 50 mM Tris-MOPS (pH 8.1), 100 mM KCl, 1% sodium cholate, and 10 μg/mL PMSF. The resulting suspension was sonicated three times for 30 s each and centrifuged at 100000*g* for 30 min, after which the supernatant was applied to a column containing HisPur Cobalt affinity resin (Thermo Scientific, Rockford, IL). The column was washed with solubilization buffer containing 15 mM imidazole and the protein eluted in solubilization buffer containing 300 mM imidazole and 10% glycerol. Concentration determination and spectrophotometric analysis were conducted using a Cary 1G scanning spectrophotometer (Varian, Palo Alto, CA). Sodium dodecyl sulfate−polyacrylamide gel electrophoresis (SDS−PAGE) was conducted using Bio-Rad 4 to 20% Tris-HCl ready made gels (Bio-Rad, Hercules, CA). Fast protein liquid chromatography (FPLC) was conducted using an Akta-prime machine equipped with a Hi-prep Sephacryl S-300 column (GE Healthcare, Piscataway, NJ) using solubilization buffer.

EPR-Monitored Redox Titrations. Redox titrations were conducted at 25 °C using a solution containing 100 μM HemG in solubilization buffer (pH 7.0) and the following redox mediator dyes at 50 μM each: methyl viologen, benzyl viologen, neutral red, safranin O, anthraquinone 2-sulfonate, phenosafranin, anthraquinone 1,5-disulfonate, 2-hydroxy-1,4-naphthoquinone, indigo disulfonate, and methylene blue. The reductant and oxidant used were sodium dithionite (20 mg/mL) and potassium ferrocyanide (50 mg/mL), respectively. HemG was fully reduced anaerobically, and titration points were taken from potentials ranging from approximately −450 to −150 mV by adding small amounts of oxidant. After each addition of oxidant, the sample was stirred and allowed to come to a stable potential, and 250 μL of sample was transferred to an anaerobic EPR tube and frozen in liquid nitrogen. Potentials were obtained using a Ag/AgCl electrode. Reported potentials were then recalculated with respect to normal hydrogen electrode (NHE) values. EPR data were then collected at 9.18 GHz with a microwave power of 20 μW, and the intensity of the semiquinone signal was quantified using double integration.

PPO Assay. PPO activity was monitored as previously described (*32*). Reaction mixtures consisted of 50 mM NaH_2PO_4 (pH 8.0), 0.2% (w/v) Tween 20, 2.5 mM glutathione, 100 nM HemG, and varying amounts of protoporphyrinogen IX and menadione. Experiments were also conducted using mesoporphyrinogen and coproporphyrinogen prepared as described for protoporphyrinogen. Activity was monitored at 37 °C by following porphyrin fluorescence with a Synergy HTI plate reader (BioTek, Winooski, VT) equipped with 528 and 545 nm bandpass filters and a 550 nm highpass filter on the excitation light and a 635 nm bandpass filter on the emission light. Data (v vs [S]) were then fitted to eq 1

$$v = V_{app}[S]/(K_{app} + [S]) \quad (1)$$

where V_{app} is the apparent maximum rate and K_{app} is the apparent Michaelis−Menten constant.

RESULTS

Protein Expression and Characterization. Sequence analysis of HemG from *E. coli* revealed that it is a member of a protein family found in the γ-proteobacteria that is part of a

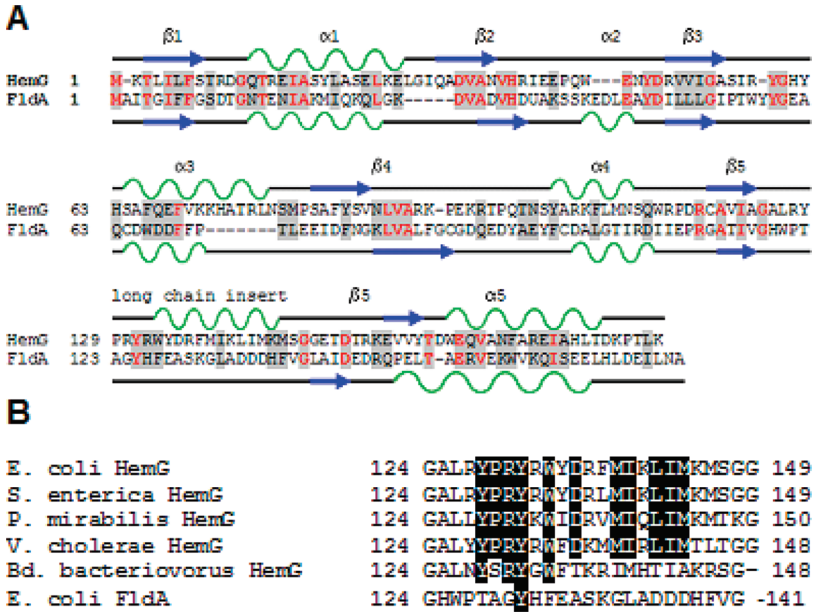

FIGURE 1: Sequence analysis of HemG. (A) Sequence and secondary structure similarity of HemG with flavodoxin A of *E. coli*. HemG is predicted by Jpred (*33*) to possess a typical flavodoxin fold motif but with one notable difference, the presence of an α-helical domain within the long chain insert loop. In the diagram, similar residues are highlighted in gray, with conserved residues colored red. α-Helices and *β*-sheets are colored green and blue, respectively, for each protein. (B) Sequence alignment of the long chain insert loop of *E. coli* HemG with that of other annotated HemG proteins and FldA. Identical residues within the predicted α helix are highlighted. A significant change in this region (i.e., *Bd. bacteriovorus*) results in a loss of function.

larger COG known as long chain flavodoxins (Figure 1) (*33*). The *hemG* gene of *E. coli* was cloned, expressed, and purified as a six-histidine-tagged recombinant protein with a yield of approximately 20 mg of protein/L of culture. A band corresponding to approximately 22 kDa was observed on SDS−PAGE (Figure 2A), which is in agreement with the theoretical value of 22.5 kDa calculated from the amino acid sequence. Matrix-assisted laser desorption ionization time-of-flight (MALDI-TOF) mass spectroscopy identified this band as HemG. A faint band located at approximately 40 kDa was identified as HemG and may represent a dimer of the protein. The cofactor was determined to be similar in size to FMN by electrospray ionization mass spectroscopy (ESI-MS). The recombinant expression plasmid rescued the HemG-deficient strain of *E. coli* SASX38, which alone cannot grow in the absence of exogenous heme.

The UV−visible spectrum of recombinant HemG possesses the expected features associated with protein and the FMN cofactor (figure 2B) along with a feature at 416 nm which probably corresponds to the Soret band of porphyrins, but it is yet to be determined if this is due to bound protoporphyrin IX. This last feature is distinct between the spectra of HemG and that of its closest relative, *E. coli* flavodoxin A, where no band is observed. Gel filtration by FPLC identified a peak corresponding to ~108 kDa suggesting that HemG exists in solution as a homotetramer.

EPR-Monitored Redox Titrations. The EPR spectra of HemG revealed a signal typical of the FMN semiquinone radical centered at $g = 2.00$. Using sodium dithionite (potential of approximately −450 mV at pH 7.0), it was possible to fully reduce the FMN. Titrations of HemG included methyl and benzyl viologens, which possess EPR signals that overlap with the FMN semiquinone radical, so the data were corrected by subtracting out the signal of the viologens alone. Data obtained at stable and reliable potentials from the double integration of interpretable spectra are shown in Figure 2C. The data were fitted to the Nernst equation (eq 2) for two consecutive one-electron redox steps:

$$[\mathrm{Fld_{sq}}]/[\mathrm{Fld_{total}}] = 1/\{1+\exp[F(E-E_2)/RT] + \exp[-F(E-E_1)/RT]\} \quad (2)$$

and normalized to the fitted maximum. E_2 and E_1 represent the first and second reduction steps of HemG and were determined to be −241 and −412 mV, respectively. These values (also shown in Figure 2C) are comparable to those of standard flavodoxins (*34*). In typical flavodoxin reactions, the semiquinone/hydroxyquinone couple is stabilized so that flavodoxins effectively function as one-electron donors or acceptors.

PPO Assays. To investigate the role of HemG in the conversion of protoporphyrinogen IX to protoporphyrin IX, HemG was assayed in the presence and absence of the potential electron acceptor, menadione, a soluble analogue of menaquinone-8. The results of this assay are shown in Figure 3A. Upon addition of excess menadione, the activity of HemG increased, reaching a rate of roughly half of that found with human PPO (3.71 and 8.54 $\mathrm{min^{-1}}$, respectively). A small amount of light-induced autoxidation occurred as indicated by the assay containing protoporphyrinogen IX only.

To provide additional evidence that HemG is a bona fide PPO, we conducted the menadione-dependent assay with the closest COG relative of HemG in *E. coli*, flavodoxin A, which cannot complement SASX38 cells, and FMN alone. Both yielded data equivalent to the rate of autoxidation seen from substrate only (results not shown). Given the high degree of similarity of HemG and FldA, these data indicate that the PPO activity of HemG is not an artifact or side reaction catalyzed by flavodoxins.

As an additional test, we cloned, expressed, and purified the long chain flavodoxin BD2899 from *Bd. bacteriovorus* that is currently annotated as a PPO. This protein is highly homologous

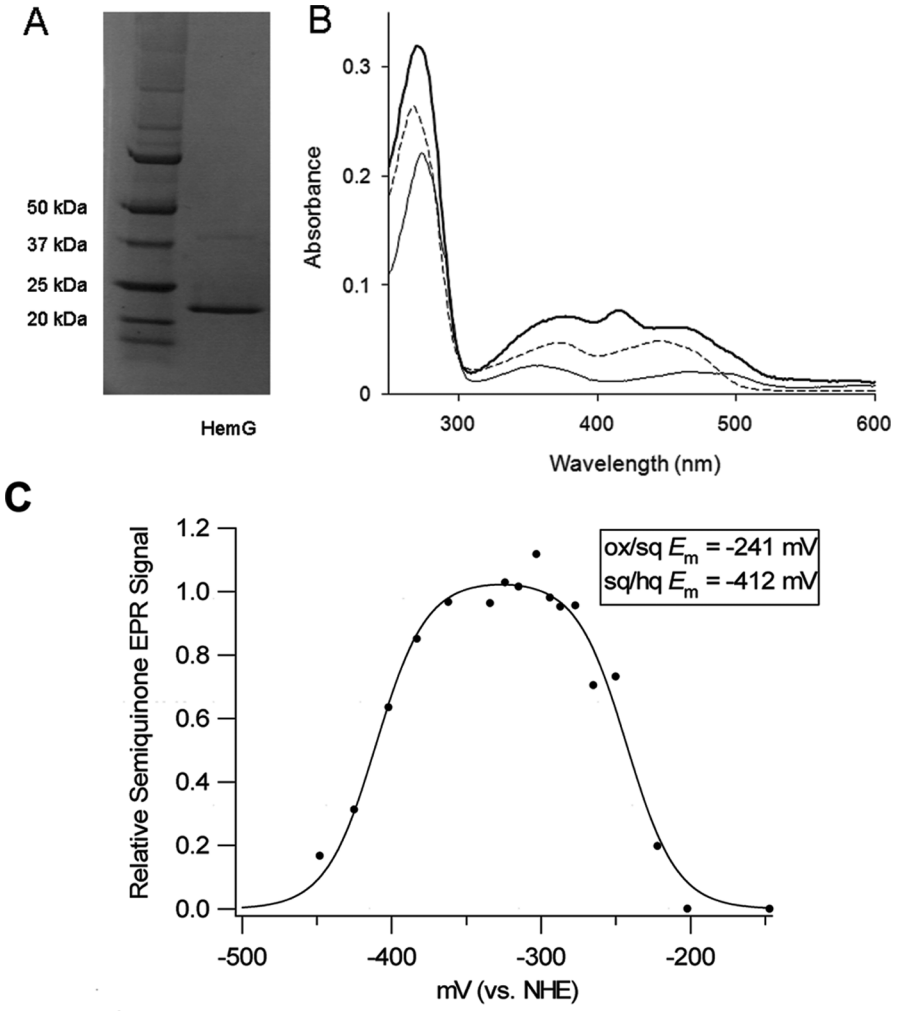

FIGURE 2: Initial characterization of HemG and its cofactor. (A) SDS−PAGE analysis of purified recombinant HemG: left lane, molecular mass markers; right lane, purified HemG. Recombinant HemG possesses a major band of approximately 22 kDa with a faint band seen at approximately 40 kDa. Both bands were identified as HemG by MS/MS analysis. (B) UV−vis spectrum analysis of purified recombinant HemG. The holoprotein (top line) exhibits characteristic FMN features (dashed line), as well as the presence of a peak at 416 nm which is lacking in *E. coli* flavodoxin A (bottom line). (C) EPR-monitored redox titration of HemG. Data were fitted to the Nernst equation for two consecutive one-electron reduction steps (eq 1). A relative semiquinone EPR signal of 1 indicates a sample in which all FMN present is in the semiquinone state. The inset shows calculated redox potentials for the oxidized/semiquinone and semiquinone/hydroxyquinone couples of the cofactor as determined with eq 1.

to HemG, including the long chain insert region (Figure 2B). However, this organism possesses the typical HemY PPO in an operon with other heme synthesizing enzyme genes, and no experimental data to support a role for this HemG-related flavodoxin in heme synthesis have been published. Interestingly, while the insert region of the *Bd. bacteriovorus* protein is more similar to that found in HemG than in FldA, it lacks an acidic residue at position 136 and a methionine at position 144 that are conserved in all other HemG forms. When expressed in the *E. coli* SASX38, this protein did not complement the *hemG* deletion.

HemG PPO activity was found to be specific for protoporphyrinogen. Neither mesoporphyrinogen nor coproporphyrinogen was oxidized by HemG. Kinetic parameters for HemG were determined for both protoporphyrinogen IX and menadione. These data are shown in Figure 3B, and the curves were fitted to the Michaelis equation (eq 2). The K_m and K_{cat} for protoporphyrinogen IX were found to be 7.0 μM and 17.52 min^{-1}, respectively, and the K_m and K_{cat} for menadione were 3.76 μM and 16.87 min^{-1}, respectively. The K_{cat}/K_m for HemG was 2.5. The kinetic parameters, along with those of other well-classified PPOs, are listed in Table 1 (*35*−*38*). The K_{cat} of HemG is slightly higher than those of most PPO enzymes, with the exception of *Desulfovibrio gigas* PPO, and the K_m for the substrate falls within the range of those of other PPOs. HemG also has a high affinity for its electron acceptor, menadione. By comparison, the reported K_m of mouse PPO for oxygen is 125 μM (*37*).

Role of the Long Chain Insert Loop. *E. coli* strain SASX38 lacks functional PPO activity and was reported to be deficient in HemG, although the nature of the mutation was never identified. In this work, sequence analysis of the SASX38 *hemG* gene revealed a deletion from nucleotide 152 to 470. This results in a predicted HemG protein that remains in frame but is lacking 106 internal amino acids, including the long chain insert loop. This long chain loop has been previously reported as being responsible for activity, specificity, and/or recognition of redox partners (*29*, *30*). Unique to HemG, this region is predicted to contain an α-helix (figure 1). Since long chain insert loops have previously been implicated in the specificity and function of flavodoxins, this region of HemG was examined by mutating the long chain insert loop of *E. coli* flavodoxin A to that of HemG. The resulting chimeric clone, FldG, was expressed in SASX38 cells deficient in HemG activity, and complementation (see the Supporting

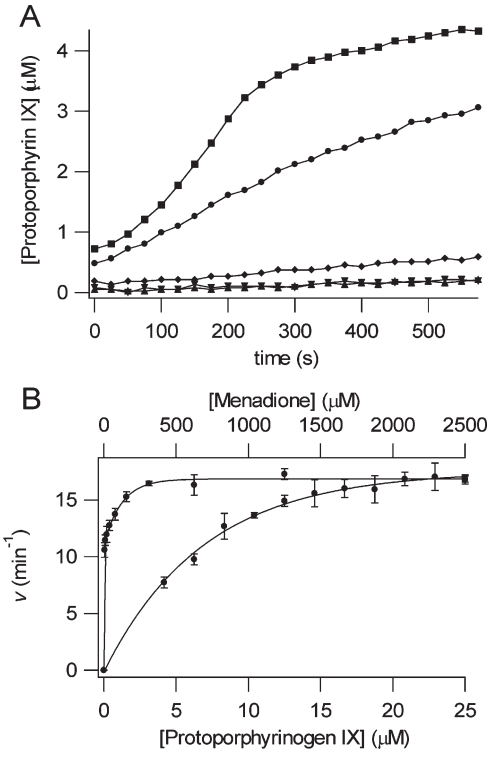

FIGURE 3: Enzymatic conversion of protoporphyrinogen IX to protoporphyrin IX by HemG. (A) PPO assays are shown for human PPO (■), 100 nM HemG and 1 mM menadione (●), 100 nM HemG (◆), 1 mM menadione (▼), and protoporphyrinogen alone (▲). In the absence of menadione, HemG is capable of generating only minimal amounts of product when compared to autoxidation. In the presence of saturating menadione concentrations, enzymatic activity is greatly increased to levels that are comparable to that of human PPO. (B) Determination of apparent Michaelis constants for HemG. HemG (100 nM) was assayed using varying concentrations of protoporphyrinogen IX (bottom curve) and menadione (top curve). Data were fitted to a single rectangular hyperbola (eq 2). K_m and K_{cat} for protoporphyrinogen IX equaled 7.0 μM and 17.52 min^{-1}, respectively; K_m and K_{cat} for menadione equaled 3.76 μM and 16.87 min^{-1}, respectively.

Table 1: Comparison of Kinetic Parameters for HemG and Various PPOs

protein	K_m (μM)	K_{cat} (min^{-1})	ref
Homo sapiens PPO	1.7/3.8	10.5/5.7	*36*
Mus musculus PPO	6.6	7.45	*37*
Bacillus subtilis PPO	1.0	0.05	*35*
D. gigas PPO	21	17.7	*38*
E. coli HemG	7.0	17.52	

Information) was obtained, indicating that in vivo the chimera can contain PPO activity. Expression and purification of the FldG protein were performed as described for HemG. Spectral analysis revealed no feature at 416 nm, and PPO assays of purified FldG showed no activity in the presence or absence of menadione.

DISCUSSION

The lack of an identifiable protoporphyrinogen oxidase in most Gram-negative bacteria represents a significant gap in our current understanding of prokaryotic heme synthesis. These organisms synthesize heme and contain all other enzymes within the pathway, so clearly an enzyme with PPO activity must exist. The dependence upon nonenzymatic conversion of protoporphyrinogen IX in vivo would be untenable since it would be unregulated and the accumulated highly reactive product would be toxic to the cell. Data presented herein clearly demonstrate that HemG is a previously uncharacterized form of PPO that is distinct from currently identified oxygen-dependent bacterial HemY PPOs. Unlike other known PPOs, HemG is a flavodoxin-based enzyme that employs menaquinone, rather than oxygen, as an electron acceptor. This is appropriate since *E. coli* is a facultative anaerobe and would be unable to synthesize heme in the absence of oxygen if it possessed a HemY type of PPO.

Because of the hydrophobicity of menaquinone and the nature of these assays, the soluble form menadione was used, which lacks the long aliphatic side chain not involved in redox properties. Our finding that HemG utilizes menadione in vitro is consistent with previous research reported by others that was conducted with cell extracts of *E. coli* (*21*−*24*). These authors found that PPO activity was associated with the respiratory chain (with fumarate, nitrate, or oxygen as the terminal electron acceptor) and the activity was localized to the membrane fraction. This location would be anticipated since the respiratory chain components, including the menaquinone-8 pool, are membrane-localized. Thus, the coupled reaction will be one in which the soluble HemG interacts with menaquinone at the membrane.

The proposition that a flavodoxin has evolved to gain function is not without precedent. WrbA, another protein similar to *E. coli* flavodoxin, possesses a quinone reductase activity much like HemG (*39*, *40*). It appears that this protein represents an evolutionary link between flavodoxins and eukaryotic NAD(P)H/quinone oxidoreductases (*41*). Like HemG, it also exists as a homotetramer, and the regions adjacent to the four FMN binding sites form an active site complex in the center of the quaternary structure (*42*, *43*). Another interesting property of WrbA and other quinone reductases in general is their ability to transfer two electrons in a ping-pong mechanism in contrast to flavodoxins which conduct one-electron reactions. This avoids the generation of semiquinone radicals that can lead to harmful reactive oxygen species (*44*). It will be of interest to determine if HemG also has the ability to function as a two-electron transfer protein. Such an ability would decrease by half the number of turnovers required to oxidize the porphyrinogen.

The data obtained from the chimeric FldG in which the long chain insert of HemG is substituted for the analogous position of flavodoxin A present possibly the most intriguing aspect of HemG. By replacing the long chain insert loop of *E. coli* flavodoxin A with the corresponding segment of HemG, we were able to complement a PPO-deficient cell line. This clearly indicates a transfer of function from HemG to a flavodoxin normally only capable of transferring electrons between redox partners. No in vitro activity with the chimera could be seen in the presence of menadione, but in vivo complementation can only occur if function is present. The lack of in vitro activity probably results from the absence of a normal flavodoxin A redox partner to accept electrons during the reaction. The most compelling reason for this is that the loop region is responsible for binding and oxidation of the tetrapyrrole but does not confer reoxidation of the cofactor by quinones. From the complementation results, it is clear that FldG is still able to interact with a physiological redox partner of FldA in vivo so that it can turn over.

Computational modeling of HemG results in a predicted structure that is similar to the typical flavodoxin motif. The predicted structure generated using 3D-JIGSAW is shown in

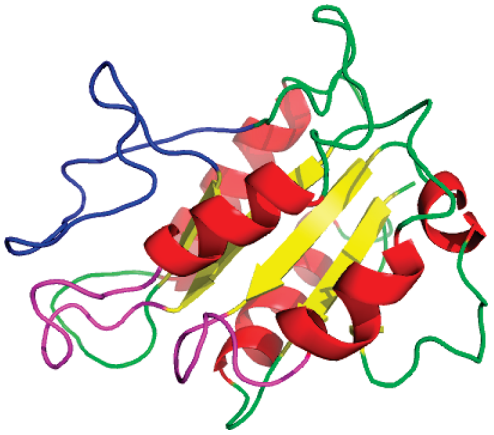

FIGURE 4: Predicted structure of HemG. This structure was generated using 3D-JIGSAW (*45*). FMN-binding loops and the long chain insert loop are colored purple and blue, respectively. The long chain insert loop sits above the binding pocket formed by the two loops allowing possible interaction with FMN.

Figure 4 (*45*). The FMN binding pocket is formed by the 50S and 90S loops, and the long chain insert loop extends behind this pocket presenting the possible interaction site for FMN and substrate, further supporting the role of the long chain insert loop.

Interestingly, the conversion of protoporphyrinogen IX to protoporphyrin IX appears to be an activity in which Gram-negative bacteria have scavenged and adapted other proteins to do the job. *Myxococcus* species contain an FAD-containing, oxygen-dependent enzyme essentially identical to eukaryotic PPOs (*17*), whereas *D. gigas* is reported to carry out catalysis using a heterotrimer complex (*38*) that remains to be characterized. HemG itself is only present in γ-proteobacteria, so the identity of PPO in the remaining Gram-negative organisms remains unknown. Thus, HemG's role as a protoporphyrinogen oxidase fills only a portion of the gap in our understanding of this point of the pathway.

There are many unanswered questions concerning HemG, its function, and the role of the long chain insert. Since it is a relatively small protein, it will be of interest to determine how it binds the substrates protoporphyrinogen and how menaquinone and catalyzes the reaction. Ongoing studies aimed at determining the X-ray crystal structure of HemG will help to answer these questions.

SUPPORTING INFORMATION AVAILABLE

SASX38 complementation was identified by the appearance of colony growth 24 h after transformation of the appropriate plasmid. In addition, the rate and extent of growth were monitored for SASX38, SASX38 with heme, SASX38 transformed with pTHHemG, and SASX38 transformed with pTHFldG. This material is available free of charge via the Internet at http://pubs.acs.org.

REFERENCES

1. Lukin, J. A., and Ho, C. (2004) The structure−function relationship of hemoglobin in solution at atomic resolution. *Chem. Rev. 104*, 1219–1230.
2. Michel, H., Behr, J., Harrenga, A., and Kannt, A. (1998) Cytochrome c oxidase: Structure and spectroscopy. *Annu. Rev. Biophys. Biomol. Struct. 27*, 329–356.
3. Munro, A. W., Girvan, H. M., McLean, K. J., Cheesman, M. R., and Leys, D. (2009) Heme and Hemoproteins. In Tetrapyrroles: Birth, Life and Death (Warren, M. J., and Smith, A. G., Eds.) pp 160−183, Landes Bioscience and Springer Science + Business Media.
4. Sun, J., Hoshino, H., Takaku, K., Nakajima, O., Muto, A., Suzuki, H., Tashiro, S., Takahashi, S., Shibahara, S., Alam, J., Taketo, M. M., Yamamoto, M., and Igarashi, K. (2002) Hemoprotein Bach1 regulates enhancer availability of heme oxygenase-1 gene. *EMBO J. 21*, 5216–5224.
5. Tahara, T., Sun, J., Igarashi, K., and Taketani, S. (2004) Heme-dependent up-regulation of the α-globin gene expression by transcriptional repressor Bach1 in erythroid cells. *Biochem. Biophys. Res. Commun. 324*, 77–85.
6. Kramer, G., Cimadevilla, J. M., and Hardesty, B. (1976) Specificity of the protein kinase activity associated with the hemin-controlled repressor of rabbit reticulocyte. *Proc. Natl. Acad. Sci. U.S.A. 73*, 3078–3082.
7. Iwai, K., Drake, S. K., Wehr, N. B., Weissman, A. M., LaVaute, T., Minato, N., Klausner, R. D., Levine, R. L., and Rouault, T. A. (1998) Iron-dependent oxidation, ubiquitination, and degradation of iron regulatory protein 2: Implications for degradation of oxidized proteins. *Proc. Natl. Acad. Sci. U.S.A. 95*, 4924–4928.
8. Raghuram, S., Stayrook, K. R., Huang, P., Rogers, P. M., Nosie A. K., McClure, D. B., Burris, L. L., Khorasanizadeh, S., Burris, T. P., and Rastinejad, F. (2007) Identification of heme as the ligand for the orphan nuclear receptors REV-ERBα and REV-ERB*β*. *Nat. Struct. Mol. Biol. 14*, 1207–1213.
9. Raspe, E., Duez, H., Mansen, A., Fontaine, C., Fievet, C., Fruchart, J. C., Vennstrom, B., and Staels, B. (2002) Identification of Rev-erbα as a physiological repressor of apoC-III gene transcription. *J. Lipid Res. 43*, 2172–2179.
10. Yin, L., Wu, N., Curtin, J. C., Qatanani, M., Szwergold, N. R., Reid, R. A., Waitt, G. M., Parks, D. J., Pearce, K. H., Wisely, G. B., and Lazar, M. A. (2007) Rev-erbα, a heme sensor that coordinates metabolic and circadian pathways. *Science 318*, 1786–1789.
11. Cho, H. Y., Cho, H. C., Kim, Y. M., Oh, J. I., and Kang, B. S. (2009) Structural insight into the heme-based redox sensing by DosS from *Mycobacterium tuberculosis*. *J. Biol. Chem. 284*, 13057–13067.
12. Torres, V. J., Stauff, D. L., Pishchany, G., Bezbradica, J. S., Gordy L. E., Iturregui, J., Anderson, K. L., Dunman, P. M., Joyce, S., and Skaar, E. P. (2007) A *Staphylococcus aureus* regulatory system that responds to host heme and modulates virulence. *Cell Host Microbe 1*, 109–119.
13. Medlock, A. E., and Dailey, H. A. (2009) Regulation of mammalian heme biosynthesis. In Tetrapyrroles: Birth, Life and Death (Warren, M. J., and Smith, A. G., Eds.) pp 116−127, Landes Bioscience and Springer Science+Business Media.
14. Hift, R. J., Meissner, P. N., Corrigall, A. V., Ziman, M. R., Petersen, L. A., Meissner, D. M., Davidson, B. P., Sutherland, J., Dailey, H. A., and Kirsch, R. E. (1997) Variegate porphyria in South Africa, 1688−1996: New developments in an old disease. *S. Afr. Med. J. 87*, 722–731.
15. Ajioka, R. S., Phillips, J. D., and Kushner, J. P. (2006) Biosynthesis of heme in mammals. *Biochim. Biophys. Acta 1763*, 723–736.
16. Panek, H., and O'Brian, M. R. (2002) A whole genome view of prokaryotic haem biosynthesis. *Microbiology 148*, 2273–2282.
17. Corradi, H. R., Corrigall, A. V., Boix, E., Mohan, C. G., Sturrock, E. D., Meissner, P. N., and Acharya, K. R. (2006) Crystal structure of protoporphyrinogen oxidase from *Myxococcus xanthus* and its complex with the inhibitor acifluorfen. *J. Biol. Chem. 281*, 38625–38633.
18. Koch, M., Breithaupt, C., Kiefersauer, R., Freigang, J., Huber, R., and Messerschmidt, A. (2004) Crystal structure of protoporphyrinogen IX oxidase: A key enzyme in haem and chlorophyll biosynthesis. *EMBO J. 23*, 1720–1728.
19. Dailey, T. A., and Dailey, H. A. (1998) Identification of an FAD superfamily containing protoporphyrinogen oxidases, monoamine oxidases, and phytoene desaturase. Expression and characterization of phytoene desaturase of *Myxococcus xanthus*. *J. Biol. Chem. 273*, 13658–13662.
20. Dailey, T. A., Meissner, P., and Dailey, H. A. (1994) Expression of a cloned protoporphyrinogen oxidase. *J. Biol. Chem. 269*, 813–815.
21. Jacobs, N. J., and Jacobs, J. M. (1978) Quinones as hydrogen carriers for a late step in anaerobic heme biosynthesis in *Escherichia coli*. *Biochim. Biophys. Acta 544*, 540–546.
22. Jacobs, J. M., and Jacobs, N. J. (1977) The late steps of anaerobic heme biosynthesis in *E. coli*: Role for quinones in protoporphyrinogen oxidation. *Biochem. Biophys. Res. Commun. 78*, 429–433.
23. Jacobs, N. J., and Jacobs, J. M. (1975) Fumarate as alternate electron acceptor for the late steps of anaerobic heme synthesis in *Escherichia coli*. *Biochem. Biophys. Res. Commun. 65*, 435–441.

24. Jacobs, N. J., and Jacobs, J. M. (1976) Nitrate, fumarate, and oxygen as electron acceptors for a late step in microbial heme synthesis. *Biochim. Biophys. Acta 449*, 1–9.
25. Hastings, S. F., Kaysser, T. M., Jiang, F., Salerno, J. C., Gennis, R. B., and Ingledew, W. J. (1998) Identification of a stable semiquinone intermediate in the purified and membrane bound ubiquinol oxidase-cytochrome bd from *Escherichia coli*. *Eur. J. Biochem. 255*, 317–323.
26. Wissenbach, U., Kroger, A., and Unden, G. (1990) The specific functions of menaquinone and demethylmenaquinone in anaerobic respiration with fumarate, dimethylsulfoxide, trimethylamine N-oxide and nitrate by *Escherichia coli*. *Arch. Microbiol. 154*, 60–66.
27. Sasarman, A., Chartrand, P., Lavoie, M., Tardif, D., Proschek, R., and Lapointe, C. (1979) Mapping of a new heme gene in *Escherichia coli* K12. *J. Gen. Microbiol. 113*, 297–303.
28. Sasarman, A., Letowski, J., Czaika, G., Ramirez, V., Nead, M. A., Jacobs, J. M., and Morais, R. (1993) Nucleotide sequence of the hemG gene involved in the protoporphyrinogen oxidase activity of *Escherichia coli* K12. *Can. J. Microbiol. 39*, 1155–1161.
29. Lopez-Llano, J., Maldonado, S., Bueno, M., Lostao, A., Angeles-Jimenez, M., Lillo, M. P., and Sancho, J. (2004) The long and short flavodoxins: I. The role of the differentiating loop in apoflavodoxin structure and FMN binding. *J. Biol. Chem. 279*, 47177–47183.
30. Lopez-Llano, J., Maldonado, S., Jain, S., Lostao, A., Godoy-Ruiz, R., Sanchez-Ruiz, J. M., Cortijo, M., Fernandez-Recio, J., and Sancho, J. (2004) The long and short flavodoxins: II. The role of the differentiating loop in apoflavodoxin stability and folding mechanism. *J. Biol. Chem. 279*, 47184–47191.
31. Dailey, H. A. (2002) Terminal steps of haem biosynthesis. *Biochem. Soc. Trans. 30*, 590–595.
32. Shepherd, M., and Dailey, H. A. (2005) A continuous fluorimetric assay for protoporphyrinogen oxidase by monitoring porphyrin accumulation. *Anal. Biochem. 344*, 115–121.
33. Cole, C., Barber, J. D., and Barton, G. J. (2008) The Jpred 3 secondary structure prediction server. *Nucleic Acids Res. 36*, W197–W201.
34. Steensma, E., Heering, H. A., Hagen, W. R., and Van Mierlo, C. P. (1996) Redox properties of wild-type, Cys69Ala, and Cys69Ser *Azotobacter vinelandii* flavodoxin II as measured by cyclic voltammetry and EPR spectroscopy. *Eur. J. Biochem. 235*, 167–172.
35. Corrigall, A. V., Siziba, K. B., Maneli, M. H., Shephard, E. G., Ziman, M., Dailey, T. A., Dailey, H. A., Kirsch, R. E., and Meissner, P. N. (1998) Purification of and kinetic studies on a cloned protoporphyrinogen oxidase from the aerobic bacterium, *Bacillus subtilis*. *Arch. Biochem. Biophys. 358*, 251–256.
36. Dailey, T. A., and Dailey, H. A. (1996) Human protoporphyrinogen oxidase: Expression, purification, and characterization of the cloned enzyme. *Protein Sci. 5*, 98–105.
37. Ferreira, G. C., and Dailey, H. A. (1988) Mouse protoporphyrinogen oxidase. Kinetic parameters and demonstration of inhibition by bilirubin. *Biochem. J. 250*, 597–603.
38. Klemm, D. J., and Barton, L. L. (1987) Purification and properties of protoporphyrinogen oxidase from an anaerobic bacterium, *Desulfovibrio gigas*. *J. Bacteriol. 169*, 5209–5215.
39. Grandori, R., Khalifah, P., Boice, J. A., Fairman, R., Giovanielli, K., and Carey, J. (1998) Biochemical characterization of WrbA, founding member of a new family of multimeric flavodoxin-like proteins. *J. Biol. Chem. 273*, 20960–20966.
40. Patridge, E. V., and Ferry, J. G. (2006) WrbA from *Escherichia coli* and *Archaeoglobus fulgidus* is an NAD(P)H:quinone oxidoreductase. *J. Bacteriol. 188*, 3498–3506.
41. Carey, J., Brynda, J., Wolfova, J., Grandori, R., Gustavsson, T., Ettrich, R., and Smatanova, I. K. (2007) WrbA bridges bacterial flavodoxins and eukaryotic NAD(P)H:quinone oxidoreductases. *Protein Sci. 16*, 2301–2305.
42. Andrade, S. L., Patridge, E. V., Ferry, J. G., and Einsle, O. (2007) Crystal structure of the NADH:quinone oxidoreductase WrbA from *Escherichia coli*. *J. Bacteriol. 189*, 9101–9107.
43. Gorman, J., and Shapiro, L. (2005) Crystal structures of the tryptophan repressor binding protein WrbA and complexes with flavin mononucleotide. *Protein Sci. 14*, 3004–3012.
44. Deller, S., Macheroux, P., and Sollner, S. (2008) Flavin-dependent quinone reductases. *Cell. Mol. Life Sci. 65*, 141–160.
45. Contreras-Moreira, B., and Bates, P. A. (2002) Domain fishing: A first step in protein comparative modelling. *Bioinformatics 18*, 1141–1142.